Computers & Fluids 38 (2009) 1580–1591

Contents lists available at ScienceDirect

Computers & Fluids

journal homepage: www.elsevier.com/locate/compfluid

Evaluation of numerical error estimation based on grid refinement studies with the method of the manufactured solutions

L. Eça [a,*], M. Hoekstra [b]

[a] Instituto Superior Técnico, Av. Rovisco Pais 1, 1049-001 Lisboa, Portugal
[b] Maritime Research Institute Netherlands, P.O. Box 28, 6700AA Wageningen, The Netherlands

ARTICLE INFO

Article history:
Received 26 November 2007
Received in revised form 11 December 2008
Accepted 14 January 2009
Available online 22 January 2009

ABSTRACT

This article presents a study on the estimation of the numerical uncertainty based on grid refinement studies with the method of manufactured solutions. The availability of an exact solution and the convergence of the numerical solution to machine accuracy allow the determination of the exact error and of the distinct contributions of the iterative and discretization errors. The study focuses on three different problems of error/uncertainty evaluation (the uncertainty is in this case the error multiplied by a safety factor): the estimation of the iterative error/uncertainty; the influence of the iterative error on the estimation of the discretization error/uncertainty, and the overall numerical error/uncertainty as a combination of the iterative and discretization errors. The results obtained in this study show that it is possible to obtain a reliable iterative error estimator based on a geometric-progression extrapolation of the L_∞ norm of the differences between iterations. In order to obtain a negligible influence of the iterative error on the estimation of the discretization error, the iterative error must be two to three orders of magnitude smaller than the discretization error. If the iterative error is non-negligible it should be added, simply arithmetically, to the discretization error to obtain a reliable estimate of the numerical error; combining by RMS is not conservative.

© 2009 Elsevier Ltd. All rights reserved.

1. Introduction

With the maturing of Computational Fluid Dynamics (CFD) codes for engineering applications comes the need to establish the credibility of the results by Verification and Validation. Because the discussion about these important subjects is ongoing in several forums, for example, the AIAA [1], the ERCOFTAC [2], the ASME [3,4], the ASCE [5], or the ITTC Resistance Committee [6], various definitions of Verification and Validation may be encountered. However, a clear and simple definition is given by Roache [7]: Verification is a purely mathematical exercise that intends to show that we are "solving the equations right", whereas Validation is a science/engineering activity that intends to show that we are "solving the right equations".

Verification is in fact composed of two different activities [7]: Code Verification and Verification of Calculations. Code Verification is to verify that a given code solves correctly the equations of the model that it contains by error evaluation. On the other hand, Verification of Calculations (or "Verification of Solutions" [4]) attempts to estimate the error of a given calculation, for which in general the exact solution is not known. Verification of Calculations should be preceded by Code Verification, a rule which was endorsed by the results of the first workshop on uncertainty analysis, held in Lisbon in 2004 [8,9].

Verification of calculations requires the estimation of the numerical error while the exact solution is unknown. In non-linear problems, typical of CFD, this is not a straightforward exercise. It is commonly accepted [7] that the numerical uncertainty (the estimated error multiplied by a safety factor) of a CFD prediction has three components: the round-off error, the iterative error and the discretization error. The round-off error is a consequence of the finite precision of the computers and its importance tends to increase with grid refinement. The iterative error stems from the non-linearity of the mathematical equations solved by CFD. In principle, one should be able to reduce the iterative error to the level of the round-off error. This may not always be feasible in complex flows though. The discretization error is a consequence of the approximations made (finite-differences, finite-volume, finite-elements, etc.) to transform the partial differential equations of the continuum formulation into a system of algebraic equations. Unlike the other two error sources, the relative importance of the discretization error decreases with the grid refinement.

For smooth solutions, the round-off error can be kept at negligible levels using 15 digits precision. The estimation of the iteration error and its influence on the estimate of the discretization error is a more complex matter. The study reported in [10] shows that the

* Corresponding author. Tel.: +351 218417992; fax: +351 218417398.
E-mail addresses: eca@marine.ist.utl.pt (L. Eça), M.Hoekstra@marin.nl (M. Hoekstra).

0045-7930/$ - see front matter © 2009 Elsevier Ltd. All rights reserved.
doi:10.1016/j.compfluid.2009.01.003

influence of the iterative error is usually underestimated. However, the study was based on test cases which do not have an exact solution, which leaves some room for dispute.

The Method of the Manufactured Solutions (MMS) [7,11–17] has in the first place been conceived for Code Verification. By providing an exact solution (though usually not a physically realistic one) the code can be checked rigorously. However, nothing prevents the use of realistic solutions in MMS. Then it turns out to be excellently suited for evaluation of methodologies for Verification of Calculations [17]. With an exact solution and a numerical solution converged to machine accuracy available, reliable evaluations of the iterative and discretization errors can be made for an intermediate numerical solution at any stage of the convergence process:

- The difference between an intermediate numerical solution and the exact solution gives the numerical error.
- The difference between an intermediate numerical solution and the solution converged to machine accuracy gives the iterative error.
- The difference between the solution converged to machine accuracy and the exact solution gives the discretization error.

Therefore, it is possible to assess the performance of procedures for iterative and discretization error estimation. Furthermore, the most reliable way to combine both sources of error when there is no dominant contribution can be evaluated with the MMS.

In this article, an evaluation is made of procedures for the estimation of the numerical uncertainty [7] for a Manufactured Solution, in particular the reasonably demanding MS which has recently been proposed for Code Verification of two-dimensional, steady, incompressible flows [18]. The iterative error estimation is based on a geometric-progression extrapolation of the difference between consecutive iterations, using the iteration counter as the independent variable [10]. A least-squares root version of the Grid Convergence Index [7], combined with use of the data range for anomalous cases, is adopted for the estimation of the discretization uncertainty [19].

Section 2 presents the procedures to estimate the iterative and discretization errors and the numerical uncertainty. For the sake of completeness, the manufactured solution is described in Section 3. The results of this study are presented and discussed in Section 4. Finally, the conclusions are summarized in Section 5.

2. Estimation of numerical errors and numerical uncertainty

The estimation of the numerical uncertainty of a CFD prediction is related to the estimation of the numerical error, but it requires an additional safety factor [20]to guarantee a 95% confidence level for the exact solution being within the estimated error bar.

As mentioned in Section 1, the numerical error of a CFD prediction has three components: the round-off error, the iterative error and the discretization error. The reduction of the round-off error is related to the number of digits available and to the numerical procedure applied to obtain the solution. In ill-conditioned problems, e.g. in complex analytical solutions defined by infinite series expansions, one may have difficulties in reducing the contribution of the round-off error. But for smooth solutions the use of double-precision is usually sufficient to avoid contamination of the error by round-off. Obviously, there is a limit imposed by the round-off error to the amount of grid refinement.

On the other hand, the reduction of the iterative error to negligible levels may be difficult and/or excessively time consuming. And if a solution has a non-negligible iterative error, it is not obvious how it should be combined with an estimated discretization error to get a reliable numerical error. With a Manufactured Solution (MS) providing the exact solution of the problem, it is possible to investigate this, to evaluate iterative and discretization errors and to verify error estimation procedures. It also provides a good environment to test how the two sources of error should be combined to obtain the numerical uncertainty (And in fact, the result obtained herein is somewhat non-intuitive).

2.1. Iterative error

The iterative error is related to the non-linearity of the system of partial differential equations solved in CFD. There are several sources of non-linearity in the Reynolds-averaged Navier–Stokes equations:

- *The convective terms:* The usual linearization procedures are Picard or Newton methods, see for example [21], which imply an iterative solution.
- *Deferred corrections in the discretization schemes of the continuity and momentum equations:* The velocity derivatives of the convective terms are often discretized with high-order schemes, but with implicit first-order approximations and explicit higher order contributions.
- *The turbulence closure:* For example, one and two-equation eddy-viscosity models have non-linear convective terms and non-linear production and dissipation terms. Also, the turbulence model equations are often solved segregated from the continuity and momentum equations.

Furthermore, the linear system of algebraic equations obtained from the discretization of the linearized partial differential equations is rarely solved with a direct method. Therefore, the solution process includes an extra iterative cycle originating from the way in which the linear systems of equations is solved. In most flow solvers, no clear distinction is made between the various iterative cycles. Therefore, in estimating the iterative error it is important to be aware of the meaning of one iteration of the solution procedure.

In principle, the iterative error may be decreased as far as the machine accuracy permits. However, in complex turbulent flows it is not guaranteed that one achieves that level of convergence. Furthermore, the c.p.u. time required to attain such level of iterative error may be significantly higher than to obtain an "acceptable" level of the iterative error. For this reason it is unusual in industrial applications of CFD to converge to machine accuracy, which brings up the need to develop reliable techniques for estimating the contribution of the iterative error to the numerical uncertainty.

An attractive way to estimate the iterative error is to use norms of the change in the solution from one iteration to the other. In this study, we have followed the experience reported in [10] and have adopted the L_∞ norm of the variable change between consecutive iterations:

$$L_\infty(\Delta\phi) = \mathrm{MAX}\left(|\phi^n - \phi^{n-1}|\right) \quad 1 \leqslant i \leqslant N_P \tag{1}$$

where N_P stands for the total number of nodes of a given grid and $\Delta\phi$ for the local change of the flow quantity ϕ. However, we have also tested the Root Mean Square (L_{RMS}) of the change between consecutive iterations,

$$L_{RMS} = \sqrt{\frac{\sum_{i=1}^{N_P}\left(\phi^n - \phi^{n-1}\right)^2}{N_P}}, \tag{2}$$

because it is often used as a convergence criterion.

The values of $L_\infty(\Delta\phi)$ and $L_{RMS}(\Delta\phi)$ obtained in any iteration n may be used as an iterative error estimator. However, our previous experience [10] shows that none of these values is a reliable itera-

tive error estimator, especially when the rate of convergence is small. Therefore, we have changed to the representation of $L_\infty(\Delta\phi)$ and $L_{RMS}(\Delta\phi)$ by a geometric progression,

$$L(\Delta\phi)|_n = L(\Delta\phi)|_{n_o} 10^{-q(n_o-n)} \tag{3}$$

with a ratio, ρ, between consecutive evaluations of $L(\Delta\phi)|_n$:

$$\rho = \frac{L_\infty(\Delta\phi)|_n}{L_\infty(\Delta\phi)|_{n-1}} = 10^q. \tag{4}$$

$L(\Delta\phi)|_{n_o}$ is the value of L_∞ or $L_{\text{RMS}}(\Delta\phi)$ at the last iteration performed, n_o, and q is related to the convergence rate. It is obvious that a convergent solution requires $\rho < 1$, i.e. $q < 0$.

Eq. (3) is equivalent to

$$L(\Delta\phi)|_n = L(\Delta\phi)|_{n_o} e^{-B(n_o-n)} \tag{5}$$

with $B = \log_{10} q$.

Applying the logarithm to both sides of Eq. (3) we obtain

$$\log(L(\Delta\phi)|_n) = \log\left(L(\Delta\phi)|_{n_o}\right) - q(n_o - n), \tag{6}$$

which defines a linear relation with two unknowns, $\log(L(\Delta\phi)|_{n_o})$ and q. It is not safe, however, to obtain q from Eq. (6) using the results of only two subsequent iterations, because there is no guarantee that the convergence is smooth.[1] Moreover, there are plenty of data available from previous iterations. Therefore, the safest way is to solve Eq. (6) in the least squares root sense using the data of the last $m+1$ iterations. Designating $\log(L(\Delta\phi)|_i)$ by $\mathscr{L}_i$, this leads to

$$q_f = \frac{(m+1)\sum_{i=n_o-m}^{n_o} i\mathscr{L}_i - \left(\sum_{i=n_o-m}^{n_o}\mathscr{L}_i\right)\left(\sum_{i=n_o-m}^{n_o} i\right)}{(m+1)\sum_{i=n_o-m}^{n_o} i^2 - \left(\sum_{i=n_o-m}^{n_o} i\right)\left(\sum_{i=n_o-m}^{n_o} i\right)} \tag{7}$$

and

$$\log(L(\Delta\phi)|_{n_{of}}) = \frac{\sum_{i=n_o-m}^{n_o}\mathscr{L}_i - q_f\sum_{i=n_o-m}^{n_o} i}{m+1} + q_f m, \tag{8}$$

where $L(\Delta\phi)|_{n_{of}}$ is the value obtained from the fit, which is not necessarily equal to $L(\Delta\phi)|_{n_o}$.

For $\rho < 1$, the sum of all terms of the geometric progression (3) with $n \geqslant n_o$ is given by

$$L(\Delta\phi)| = \frac{L(\Delta\phi)|_{n_{of}}}{1 - 10^{q_f}}, \tag{9}$$

which represents an extrapolated estimate of the iterative error.

In some cases, the convergence may not be very smooth. The standard deviation of the fit:

$$D_f = \sqrt{\frac{\sum_{i=n_o-n}^{n_o}\left(\mathscr{L}_i - \left(\log\left(L(\Delta\phi)|_{n_{of}}\right) + q_f(n-n_o)\right)\right)^2}{n-1}}. \tag{10}$$

is significant then, and it may be used to obtain a more conservative estimate of the iterative error [10].

Here, we have tested two iterative error estimators:

(1) The extrapolation of $L_\infty(\Delta\phi)$ with Eq. (9), $e_{i\infty}$.
(2) The extrapolation of $L_{RMS}(\Delta\phi)$ with Eq. (9), e_{iRMS}.

In both cases, we include the corrections based on the influence of the standard deviation of the fit, D_f.

The results obtained using the maximum differences obtained in the last iteration performed as the iterative error estimators are reported in [22].

[1] We recall that several iterative cycles may be contained in one iteration of the solution procedure.

2.1.1. Contribution of the iterative error to the numerical uncertainty

In our previous exercises [10], we have used the iterative error estimators directly as the contribution of the iterative error to the numerical uncertainty: In this study, we have tested two alternatives:

(1) Use the iterative error estimators, e_i, as they come.
(2) Multiply e_i by a safety factor of 1.25: $U_i = 1.25e_i$.

For every grid of each test case, the numerical solution was converged to machine accuracy. Therefore, we can make an almost exact estimate of the iterative error for the solutions obtained with less demanding convergence criteria. We will designate the iterative error obtained from the difference to the solution converged to machine accuracy by e_{im}.

In this study we compare e_{im} with four quantities: $e_{i\infty}, e_{iRMS}, U_{i\infty}$ and U_{iRMS}.

2.1.2. Monitoring the iterative error

In the assessment of the performance of iterative error estimators there are plenty of data available. What is needed, though, is a meaningful measure to judge the performance of the iterative error estimators. In this study, we have computed the following quantities:

- The ratio between the iterative error/uncertainty estimator, e_i or U_i, and the iterative error obtained from the difference to the solution converged to machine accuracy, e_i/e_{im}.
- The percentage of grid nodes where the iterative error/uncertainty estimator is smaller than e_{im}, ($e_i < e_{im}$ or $U_i < e_{im}$), represented by the symbol F.

The quality of the iterative error/uncertainty estimator is indicated by the ratio e_i/e_{im}. An optimal error estimator would have e_i/e_{im} equal to one. If this value is smaller than one the error estimator does not bound the iterative error on all the grid nodes. On the other hand, a value much larger than one indicates that the error estimation is too conservative, which may unjustly penalize the uncertainty estimation. In this study, we have computed the minimum value of e_i/e_{im}. In the selected test case (a manufactured solution that mimics a turbulent boundary-layer) the maximum value of this ratio may not be very significant, because e_i is estimated for all grid nodes and e_{im} may vary by orders of magnitude in the computational domain.

If the error/uncertainty estimator fails to bound the iterative error, ($(e_i/e_{im})_{min} < 1$ or $(U_i/e_{im})_{min} < 1$), F quantifies the percentage of grid nodes where the estimate fails.

2.2. Contribution of the discretization error to the numerical uncertainty

The basis of the procedure for the estimation of the discretization uncertainty, U_d, of the solution of an integral or local flow quantity on a given grid is the standard Grid Convergence Index (GCI) method [7], which relies on error estimation using Richardson extrapolation.

$$\delta_{RE} = \phi_i - \phi_o = \alpha h_i^p, \tag{11}$$

where ϕ_i is the numerical solution of any local or integral scalar quantity on a given grid (designated by the subscript i), ϕ_o is the estimated exact solution, α is a constant, h_i is a parameter which identifies the representative grid cell size and p is the observed order of accuracy. However, α, p and ϕ_o are obtained in the least squares root sense [23]using the data of at least four grids (instead of the grid triplet of the original GCI).

The ability to estimate the error with Richardson extrapolation depends on the apparent convergence condition, being one of the following options:

- Monotonic convergence.
- Oscillatory convergence.
- Monotonic divergence.
- Oscillatory divergence.

When Richardson extrapolation is performed in the least squares sense the determination of the apparent convergence condition is not as straightforward as for a single grid triplet [7] (especially for a constant grid refinement ratio, i.e. $h_2/h_1 = h_3/h_2$) because the data may exhibit scatter [23]. First, we establish the apparent order of convergence p from the least squares fit to ϕ to determine the cases of apparent monotonic convergence ($p > 0$) or divergence ($p < 0$). If there is no p that fits the data, we determine p' from a fit to $\phi'_i = |\phi_{i+1} - \phi_i|$ to determine the cases of oscillatory convergence ($p' > 0$) or divergence ($p' < 0$). If it is impossible to determine p or p', we assume that we have oscillatory convergence.

The only condition which allows an error estimation based on Richardson extrapolation is monotonic convergence. In other cases one must rely on alternative uncertainty quantification, which we have chosen to be based (also) on the maximum difference between all the solutions available, Δ_M,

$$\Delta_M = \max\left(|\phi_i - \phi_j|\right) \quad \text{with} \quad 1 \leqslant i \leqslant n_g \wedge 1 \leqslant j \leqslant n_g. \tag{12}$$

In the last few years, we have tested several procedures for the uncertainty estimation based on the GCI using δ_{RE} and Δ_M. The goal is to obtain an error band for a given calculation result such that the exact solution is within that band with 95% confidence. The present version of the procedure is a result of the experience obtained in a variety of test cases and the suggestions and comments of the first Workshop on CFD Uncertainty Analysis held in Lisbon in October 2004 [8]. It starts with the evaluation of the observed order p. If p is between 1 and 2 we apply the GCI with the proposed safety factor of 1.25. If $p < 1$, δ_{RE} tends to become over-conservative[2] and so we take the minimum of δ_{RE} and Δ_M as the error estimator.

For super-convergence, i.e. p higher than the theoretical order of the method, the values of δ_{RE} are not reliable. In most of these cases, the observed super-convergence is not real and is merely a consequence of the numerical shortcomings[3] affecting the determination of p. If more than three grids are available, this is easily identified from the very strong dependence of p on the data points selected. Therefore, in case of super-convergence we perform the Richardson extrapolation with p replaced by its theoretical value to obtain the error estimator. So we introduce δ^*_{RE}, which for a nominally second-order method is:

$$\delta^*_{RE} = \phi_i - \phi_o = \alpha h_i^2. \tag{13}$$

Eq. (13) is also solved via a least squares approximation and the uncertainty is obtained from the maximum of the values based on δ^*_{RE} and Δ_M.

In principle, if the code has been verified, i.e. there are no bugs in the implementation of the numerical model, one should not expect to obtain divergent situations, unless the data are outside the asymptotic range. Therefore, in all cases where the data do not exhibit monotonic convergence we determine the uncertainty by multiplying Δ_M with a factor of safety of 3. With our 95% confidence level in mind, this seems an acceptable guess [8], but requires further corroboration.

We can summarize our procedure for the estimation of the numerical uncertainty, valid for a nominally second-order accurate method, as follows:

(1) The observed order of accuracy is estimated with the least squares root technique to identify the apparent convergence condition according to the definition given above.
(2) For monotonic convergence:

- For $0.95 \leqslant p < 2.05$

$$U_d(\phi) = 1.25\delta_{RE} + U_s.$$

- For $0 < p < 0.95$

$$U_d(\phi) = \min(1.25\delta_{RE} + U_s, 1.25\Delta_M).$$

- For $p \geqslant 2.05$

$$U_d(\phi) = \max(1.25\delta'_{RE} + U_s, 1.25\Delta_M).$$

(3) If monotonic convergence is not observed:

$$U_d(\phi) = 3\Delta_M$$

The procedure assumes the iterative and round-off errors to be negligible, and the data to be in the so-called asymptotic range (to justify the use of (11)). The tests performed in this study include data with non-negligible iterative errors and grids of different densities. The aim is to investigate the influence of these two "perturbations" in the outcome of the discretization uncertainty estimation performed with the procedure described above.

2.3. Numerical uncertainty

In this section, we will assume that the round-off error is negligible compared with the discretization and iterative contributions to the numerical uncertainty, U. In all our previous exercises, see for example [19] and [23], we have converged the solutions to machine accuracy. Therefore, in those cases we have $U \simeq U_d$. In practical calculations, the iterative error may not be negligible and so the numerical uncertainty will have contributions from the iterative and discretization errors.

Stern et al. [24] propose the following expression for the numerical uncertainty:

$$U = \sqrt{(U_d)^2 + (U_i)^2}, \tag{14}$$

which basically assumes that the two sources of uncertainty are independent.

This independency can be verified here, because the MMS permits precise evaluation of the total numerical error as well as reliable independent estimation of the iterative and the discretization errors. Therefore, we have checked the following relations:

$$e \leqslant \sqrt{(e_{de})^2 + (e_{im})^2}, \tag{15}$$

and

$$e \leqslant e_{de} + e_{im}. \tag{16}$$

e stands for the numerical error, e_{de} for the discretization error and e_{im} for the iterative error. In a given grid, e is computed from the difference between the numerical solution and the exact solution; the discretization error is obtained from the difference between the solution converged to machine accuracy and the

[2] δ_{RE} tends to infinity when p goes to 0.
[3] These shortcomings include the existence of scatter in the data and the possibility of the data being outside the asymptotic range.

exact solution; e_{im} is the difference to the solution converged to machine accuracy.

In general, e_d and e_i are not available, so one has to work with the estimated uncertainties, U_d and U_i. However, we have compared U_i and U_d separately. Therefore, if we have uncertainties that band the discretization and iterative errors and choose the correct way to combine both contributions, we will obtain a good numerical error estimator.

3. Manufactured solution

The present manufactured solution was proposed in [18] and [25]. It resembles a near-wall turbulent flow and includes manufactured solutions for a choice of eddy-viscosity turbulence models. In this study, we have selected the baseline (BSL) modification of the Wilcox $k-\omega$ model [26,27] proposed by Menter [28].

3.1. Computational domain and flow conditions

The computational domain is a square of side $0.5L$ with $0.5L \leqslant X \leqslant L$ and $0 \leqslant Y \leqslant 0.5L$ and the proposed Reynolds number, Rn, is 10^6

$$Rn = \frac{U_1 L}{\nu}, \tag{17}$$

where U_1 is the reference velocity, L the reference length and ν the kinematic viscosity. In non-dimensional variables, (x, y), the computational domain is given by $0.5 \leqslant x \leqslant 1$ and $0 \leqslant y \leqslant 0.5$, where x stands for the horizontal direction and y for the vertical direction.

3.2. Main flow variables

The velocity components in the x direction, u_x, and y direction, u_y, are given by

$$u_x = \mathrm{erf}(\eta) \quad \text{and} \quad u_y = \frac{1}{\sigma\sqrt{\pi}}\left(1 - e^{-\eta^2}\right). \tag{18}$$

η is a "similarity variable"

$$\eta = \frac{\sigma y}{x}, \tag{19}$$

where we have set $\sigma = 4$. Notice that with the choice (18) the continuity equation is satisfied identically.

The pressure coefficient (i.e. the pressure relative to twice the reference dynamic pressure) is given by

$$C_p = \frac{P}{\rho(U_1)^2} = 0.5\ln\left(2x - x^2 + 0.25\right)\ \ln\left(4y^3 - 3y^2 + 1.25\right) \tag{20}$$

3.3. Turbulence quantities

In the two-equation BSL k–ω turbulence model the eddy-viscosity is given by

$$\nu_t = \frac{k}{\omega} \tag{21}$$

In the selected MS [18], analytical expressions are provided for ν_t and k. The ω field is derived from Eq. (21).

$$\nu_t = 0.25(\nu_t)_{max}\eta_v^4 e^{2-\eta_v^2}, \tag{22}$$

$$k = k_{max}\eta_v^2 e^{1-\eta_v^2}, \tag{23}$$

$$\omega = 4\frac{k_{max}}{\nu_{max}} e^{-1}\eta_v^{-2}, \tag{24}$$

where $(\nu_t)_{max} = 10^3\nu$.

The BSL model includes a blending function, F_1, which does not have well-defined derivatives in the complete flow field, as discussed in [18]. Therefore, in the present exercise, the dependency of the constants σ_k and σ_ω on F_1 has been removed: $\sigma_k = \sigma_\omega = 2$.

4. Results

All calculations were performed with the 2D finite-difference version of PARNASSOS [29]that solves the steady, incompressible, RANS equations without any transformation of the continuity equation.

Theoretically, PARNASSOS is a second-order method. All the discretization schemes applied to the continuum equations are at least second-order accurate. Third-order upwind discretization is applied to the convective terms (including the transport equations of turbulence quantities). Although flux limiters are available in the code, all the present calculations were performed without flux limiters.

We have made two sets of calculations. In the first one, the eddy-viscosity, ν_t, is taken from the manufactured solution, whereas for the second the k and ω transport equations of the BSL model [28] are solved to obtain ν_t. In both cases, the iterative and discretization error/uncertainty were estimated for the two Cartesian velocity components, u_x and u_y, and for the pressure coefficient, C_p. In this article, we will focus only on the results including the numerical solution of the k and ω transport equations. Detailed results of the two exercises are reported in [22].

4.1. Boundary conditions

The MS is flexible with regard to the choice of boundary conditions. We have chosen to stay close to normal practice in the simulation of near-wall turbulent flows. If the subscript ms identifies the MS solution, the boundary conditions applied to the horizontal velocity component, u_x, vertical velocity component, u_y, and the pressure coefficient, C_p, are:

- Bottom boundary, $y = 0$:

$$u_x = (u_x)_{ms} = 0, \quad u_y = (u_y)_{ms} = 0.$$

- Inlet boundary, $x = 0.5$:

$$u_x = (u_x)_{ms}, \quad u_y = (u_y)_{ms}.$$

- Top boundary, $y = 0.5$:

$$u_x = (u_x)_{ms}, \quad C_p = (C_p)_{ms} = 0.$$

- Outlet boundary, $x = 1$:

$$\frac{\partial u_x}{\partial x} = \left(\frac{\partial u_x}{\partial x}\right)_{ms}, \quad \frac{\partial u_y}{\partial x} = \left(\frac{\partial u_y}{\partial x}\right)_{ms} C_p = (C_p)_{ms}.$$

The "numerical" boundary conditions required for u_y at the top boundary and C_p at the inlet and bottom boundaries were imposed using the first or second derivatives available from the MS. In PARNASSOS virtual grid nodes outside the computation domain are added for the implementation of the boundary conditions. The variable values in these virtual grid nodes were filled-in numerically, i.e. the dependent variables at the virtual nodes were not defined from the MS.

At the bottom, inlet and top boundaries k is specified from the MS. At the outlet boundary, the first derivative of k is imposed from the manufactured solution. Equivalent boundary conditions are imposed on ω with the exception of the bottom where ω tends to infinity. To avoid any contamination of the results by this awkward boundary condition, ω is specified from the MS in the first two-layers of grid nodes away from the boundary.

4.2. Grid set

The present MS has been computed with the BSL k–ω model for different types of grids including non-orthogonal curvilinear grids [30]. In this study, we will restrict ourselves to a single set of Cartesian grids. The grids have equidistant grid node distributions in the x direction, but in the y direction the grid is clustered towards the bottom boundary using a one-sided stretching function [31] (stretching parameter 0.05, i.e. the distance of the first grid node to the bottom is 0.05 times smaller than in the equidistant grid).

The grid set includes 18 geometrically similar grids covering a grid refinement ratio of 6.67. It has long since been recognized [7]that departures from strict grid similarity can pollute Richardson Extrapolation and uncertainty estimators like the GCI; the importance has been clarified by Salas [32]. The finest grid has 401×401 grid nodes and the coarsest grid 61×61. There are 19×19 physical locations which are common to all grids. This allows the determination of the convergence properties of local flow quantities without interpolation. The determination of the typical cell size, h, is straightforward.

$$h_i = \frac{1}{NX} = \frac{1}{NY}.$$

NX and NY stand for the number of nodes in the x and y directions.

4.3. Initial conditions

The RANS equations are solved iteratively because of their non-linear character. Therefore, an initial condition is required to start the calculation. In the MMS, the exact solution is an excellent candidate for the initial solution. However, such condition is not suitable for a study on the behaviour of the iterative error.

In all the calculations, the initial flow field is obtained copying the flow quantities at the inlet boundary to all parallel grid lines. For the turbulence quantities, k and ω, the initial conditions are specified from the MS.

4.4. Convergence criteria

The convergence criterion of PARNASSOS, e_t, is based on the maximum difference between consecutive iterations. One iteration of PARNASSOS includes the following steps:

(1) Determination of the eddy-viscosity.
   (a) Update of the coefficients of the discretized k and ω transport equations using the available flow quantities.
   (b) Solution of the discretized k and ω transport equations to a specified tolerance.
   (c) Update of the eddy-viscosity field from the new values of k and ω.
(2) Update of the coefficients of the discretized continuity and momentum equations with the available flow quantities.
(3) Solution of the algebraic system of the coupled equations to a specified tolerance.
(4) Update of the flow field.

In general, the tolerances for the solution of the linear systems of equations are less demanding than e_t. For the solution of the algebraic systems of equations obtained from the discretized continuity and momentum equations or the discretized k and ω transport equations, we have adopted the following convergence criteria:

- The calculation is stopped when the pre-conditioned residual drops 10 orders of magnitude.
- The maximum number of GMRES iterations allowed is 50.

The calculation stops when the maximum difference of u_x and u_y between consecutive iterations is below e_t and the maximum pressure coefficient difference between consecutive iteration is below $0.1e_t$, i.e.

$$(\Delta u_x)_{max} < e_t \wedge (\Delta u_y)_{max} < e_t \wedge (\Delta C_p)_{max} < 0.1e_t, \tag{25}$$

where $C_p = (p - p_{ref})/(\rho U_{ref}^2)$.

For the 18 grids of the set, we have stored the flow field for 13 different values of e_t. The lowest value is $e_t = 5 \times 10^{-14}$ that corresponds to machine accuracy. The remaining 12 values are $10^{-N}, N = 1,2,\ldots,12$.

4.5. Convergence histories

The maximum differences of u_x, u_y and C_p, respectively, are plotted as a function of the iteration counter in Fig. 1. The convergence of the three main flow variables is similar. As expected, the convergence rate decreases with the grid refinement. However, for NX and NY below 200 the increase of the number of iterations to attain machine accuracy with the decrease of h is very moderate, probably due to the interaction of the GMRES algebraic tolerances.

For the finest grids, there are some irregularities in the maximum differences obtained in the initial iterations. However, for a given grid, the convergence rate (which is related to the slope of the lines plotted in Fig. 1) is fairly constant for most of the iterations performed. In the coarsest grid, 61×61, there is a strange decrease of the convergence rate in the last iterations performed. This phenomenon may be avoided by changing the under-relaxation parameters used in the calculations. However, in this study we have kept these parameters fixed for all the calculations.

It may be mentioned that even without using the available exact solution it is possible to improve substantially the initial guess of the finest grids calculations. For example, in the 201×201 grid the initial condition can be generated by a simple interpolation in the converged 101×101 grid. Such strategy would reduce the number of iterations required to attain machine accuracy in the finest grids.

4.6. Iterative error estimation

The geometric-progression extrapolations (Eq. (9)) were made with all the data available for $e_t = 10^{-1}$ and $e_t = 10^{-2}$. For $e_t = 10^{-3}$ and $e_t = 10^{-4}$, the iterations needed to reach $e_t = 10^{-1}$ were discarded. For the remaining levels of e_t ($e_t \leqslant 10^{-5}$), we have used only data of the iterations performed after satisfying $e_t = 10^{-2}$.

As an example of the results obtained, Tables 1 and 2 present the values of $\text{Log}_{10}((U_{i\infty}/e_{im})_{min})$, $F_{U_{i\infty}}$, $\text{Log}_{10}((U_{iRMS}/e_{im})_{min})$ and $F_{U_{iRMS}}$ for the vertical velocity component, u_y, in the 18 grids tested at the 12 levels of e_t. Results for the all the iterative error estimators tested are reported in [22].

The iterative error estimator based on the geometric-progression extrapolation of the L_∞ norm of the differences between consecutive iterations is the most reliable iterative error estimator tested. This is in agreement with the study reported in [10]. Furthermore, the trends observed for the different iterative error estimators tested are consistent with the observations made in [10]:

- The number of cases where $e_{i\infty}$ fails to bound the iterative error is below 5% for almost all the combinations of NX and e_t. Nevertheless, there are a few exceptions for the vertical velocity component, u_y. In those cases, the safety factor reduces the percentage of failures to values below 5% for most of the cases. However, all the exceptions but one are obtained for $e_t = 10^{-1}$, which corre-

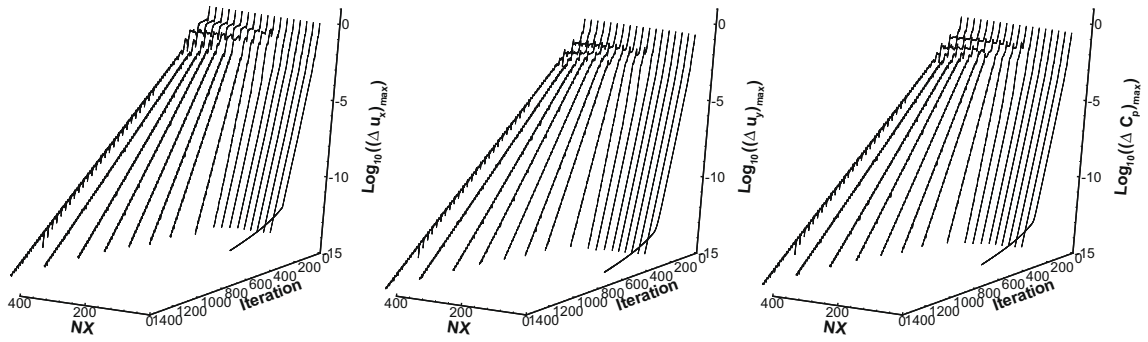

Fig. 1. Convergence of the velocity components, u_x and u_y, and pressure coefficient, C_p, in the calculations performed with the BSL $k-\omega$ model.

Table 1
$\mathrm{Log}_{10}((U_{i\infty}/e_{im})_{min})$ and $F_{U_{i\infty}}$ for the vertical velocity component, u_y as a function of the grid refinement level, h, and the convergence criteria, e_t.

$1/h$	e_t											
	−1	−2	−3	−4	−5	−6	−7	−8	−9	−10	−11	−12
$\mathrm{Log}_{10}((U_{i\infty}/e_{im})_{min})$												
400	1.68	1.35	1.15	0.95	1.10	1.01	0.88	1.05	0.91	1.08	1.17	0.89
380	1.72	1.49	1.19	0.85	0.82	0.71	0.80	0.81	0.79	0.90	0.78	0.74
360	1.70	1.54	1.15	0.79	0.77	0.91	0.74	0.74	0.74	0.61	0.79	0.69
340	1.69	1.30	1.24	0.79	0.66	0.94	0.64	0.76	0.64	0.76	0.61	0.71
320	1.38	1.61	1.17	0.61	0.58	0.56	0.53	0.55	0.54	0.53	0.52	0.51
300	1.56	1.66	1.16	0.72	0.67	0.67	0.50	0.84	0.65	0.65	0.64	0.47
280	1.21	1.28	1.24	0.58	0.57	0.76	0.58	0.54	0.53	0.56	0.56	0.50
260	−0.08	1.66	1.65	0.47	0.44	0.43	0.59	0.63	0.42	0.42	0.38	0.60
240	−0.36	1.63	1.92	0.40	0.43	0.38	0.40	0.31	0.28	0.25	0.18	0.07
220	−0.26	1.63	2.44	0.23	−0.26	0.00	0.14	0.26	0.30	0.33	0.45	0.47
200	−0.24	1.26	2.02	−0.09	−0.06	0.25	0.41	0.41	0.37	0.39	0.36	0.41
180	−0.06	0.46	0.00	−0.30	−0.16	−0.12	−0.15	−0.06	0.02	0.08	0.15	0.17
160	0.00	0.06	−0.14	−0.21	−0.15	−0.04	−0.05	−0.10	0.01	0.07	0.07	0.10
140	0.04	0.14	−0.02	−0.09	−0.04	−0.03	−0.04	−0.05	0.06	0.11	0.11	0.12
120	0.07	0.16	0.04	0.01	0.05	0.04	0.01	−0.01	0.03	0.14	0.14	0.12
100	0.11	0.26	0.07	0.02	0.11	0.08	0.00	0.03	0.06	0.11	0.16	0.20
80	−0.01	0.25	0.09	0.09	0.05	0.09	0.01	0.05	0.08	0.12	0.12	0.14
60	0.00	0.24	0.12	0.07	0.05	0.04	0.03	0.07	0.13	0.11	−0.74	−1.32
$F_{U_{i\infty}}$												
400	0.0	0.0	0.0	0.0	0.0	0.0	0.0	0.0	0.0	0.0	0.0	0.0
380	0.0	0.0	0.0	0.0	0.0	0.0	0.0	0.0	0.0	0.0	0.0	0.0
360	0.0	0.0	0.0	0.0	0.0	0.0	0.0	0.0	0.0	0.0	0.0	0.0
340	0.0	0.0	0.0	0.0	0.0	0.0	0.0	0.0	0.0	0.0	0.0	0.0
320	0.0	0.0	0.0	0.0	0.0	0.0	0.0	0.0	0.0	0.0	0.0	0.0
300	0.0	0.0	0.0	0.0	0.0	0.0	0.0	0.0	0.0	0.0	0.0	0.0
280	0.0	0.0	0.0	0.0	0.0	0.0	0.0	0.0	0.0	0.0	0.0	0.0
260	1.5	0.0	0.0	0.0	0.0	0.0	0.0	0.0	0.0	0.0	0.0	0.0
240	27.5	0.0	0.0	0.0	0.0	0.0	0.0	0.0	0.0	0.0	0.0	0.0
220	14.1	0.0	0.0	0.0	4.9	0.0	0.0	0.0	0.0	0.0	0.0	0.0
200	14.3	0.0	0.0	2.6	0.3	0.0	0.0	0.0	0.0	0.0	0.0	0.0
180	2.9	0.0	0.0	5.2	1.3	0.6	0.6	0.2	0.0	0.0	0.0	0.0
160	0.0	0.0	3.6	3.2	1.1	0.2	0.2	0.4	0.0	0.0	0.0	0.0
140	0.0	0.0	0.2	1.2	0.3	0.2	0.2	0.2	0.0	0.0	0.0	0.0
120	0.0	0.0	0.0	0.0	0.0	0.0	0.0	0.0	0.0	0.0	0.0	0.0
100	0.0	0.0	0.0	0.0	0.0	0.0	0.0	0.0	0.0	0.0	0.0	0.0
80	0.6	0.0	0.0	0.0	0.0	0.0	0.0	0.0	0.0	0.0	0.0	0.0
60	0.0	0.0	0.0	0.0	0.0	0.0	0.0	0.0	0.0	0.0	6.8	35.8

sponds to an unreasonable level for the convergence criterion, or to the coarsest grid with the lowest values of e_t where a strange behaviour of the convergence rate is observed (see Fig. 1).

- The minimum value of the ratio between the iterative uncertainties estimated with the geometric progression extrapolation, $U_{i\infty}$, and e_{im} is larger than 1 but smaller than 10 for most of the cases tested. This is an important result because it shows that $U_{i\infty}$ does not overestimate the iterative error by orders of magnitude.
- The L_{RMS} norm is not a good iterative error estimator, even when the geometric-progression extrapolation is applied. In the present exercise, the RMS-based iterative error estimator fails essentially for the pressure coefficient and the application of a safety factor does not improve the situation significantly.
- The iterative error estimators based on the L_∞ and L_{RMS} norms of the differences obtained in the last iteration performed are not reliable. The application of a safety factor does not improve the performance of these iterative error estimators. The data

Table 2
$\mathrm{Log}_{10}((U_{iRMS}/e_{im})_{min})$ and $F_{U_{iRMS}}$ for the vertical velocity component, u_y as a function of the grid refinement level, h, and the convergence criteria, e_t.

$1/h$	e_t											
	−1	−2	−3	−4	−5	−6	−7	−8	−9	−10	−11	−12
$R_{U_{iRMS}}$												
400	1.03	1.64	0.81	0.44	0.59	0.50	0.37	0.54	0.40	0.57	0.65	0.36
380	1.06	1.54	0.97	0.38	0.34	0.23	0.32	0.32	0.31	0.42	0.29	0.25
360	1.02	1.51	0.88	0.33	0.31	0.45	0.28	0.28	0.28	0.15	0.33	0.23
340	0.95	1.18	0.87	0.45	0.29	0.57	0.27	0.39	0.26	0.39	0.23	0.33
320	1.92	1.31	0.79	0.36	0.33	0.31	0.28	0.29	0.28	0.27	0.26	0.25
300	1.74	1.45	0.93	0.51	0.43	0.43	0.26	0.60	0.41	0.41	0.40	0.22
280	1.07	1.22	1.31	0.44	0.39	0.57	0.39	0.35	0.33	0.36	0.36	0.30
260	0.08	1.29	1.15	0.28	0.23	0.22	0.38	0.42	0.21	0.21	0.16	0.39
240	−0.10	1.25	1.44	0.31	0.32	0.27	0.28	0.19	0.16	0.12	0.04	−0.10
220	−0.01	1.32	2.09	0.18	−0.44	−0.50	−1.05	−1.07	−1.01	−0.96	−0.86	−0.88
200	0.14	1.06	1.67	0.01	−1.10	−1.04	−0.76	−0.68	−0.70	−0.70	−0.79	−0.82
180	0.26	0.73	−0.51	−1.40	−1.17	−1.18	−1.33	−1.35	−1.32	−1.31	−1.32	−1.38
160	0.08	0.38	−1.11	−0.67	−0.73	−0.79	−0.95	−1.16	−1.16	−1.23	−1.35	−1.46
140	0.01	0.25	−0.95	−0.74	−0.68	−0.78	−0.91	−1.04	−1.06	−1.14	−1.28	−1.41
120	−0.05	0.13	−0.86	−0.64	−0.53	−0.64	−0.78	−0.94	−1.04	−1.07	−1.22	−1.38
100	−0.07	0.14	−0.76	−0.66	−0.44	−0.54	−0.76	−0.86	−0.96	−1.06	−1.15	−1.27
80	−0.18	0.17	−0.61	−0.67	−0.55	−0.57	−0.76	−0.85	−0.96	−1.07	−1.23	−1.36
60	−0.19	0.24	−0.65	−0.81	−0.71	−0.76	−0.86	−0.95	−1.02	−1.18	−2.18	−2.35
$F_{U_{iRMS}}$												
400	0.0	0.0	0.0	0.0	0.0	0.0	0.0	0.0	0.0	0.0	0.0	0.0
380	0.0	0.0	0.0	0.0	0.0	0.0	0.0	0.0	0.0	0.0	0.0	0.0
360	0.0	0.0	0.0	0.0	0.0	0.0	0.0	0.0	0.0	0.0	0.0	0.0
340	0.0	0.0	0.0	0.0	0.0	0.0	0.0	0.0	0.0	0.0	0.0	0.0
320	0.0	0.0	0.0	0.0	0.0	0.0	0.0	0.0	0.0	0.0	0.0	0.0
300	0.0	0.0	0.0	0.0	0.0	0.0	0.0	0.0	0.0	0.0	0.0	0.0
280	0.0	0.0	0.0	0.0	0.0	0.0	0.0	0.0	0.0	0.0	0.0	0.0
260	0.0	0.0	0.0	0.0	0.0	0.0	0.0	0.0	0.0	0.0	0.0	0.0
240	8.5	0.0	0.0	0.0	0.0	0.0	0.0	0.0	0.0	0.0	0.0	0.2
220	0.1	0.0	0.0	0.0	10.3	8.4	26.0	21.5	14.3	11.4	7.8	7.0
200	0.0	0.0	0.0	0.0	30.5	22.3	12.0	8.7	7.5	6.5	6.7	6.2
180	0.0	0.0	10.0	44.2	27.8	23.1	27.3	24.6	18.6	15.7	15.2	15.0
160	0.0	0.0	42.5	12.5	11.1	12.3	16.3	18.1	15.4	14.3	15.7	16.6
140	0.0	0.0	30.1	16.3	13.1	14.0	16.1	16.2	13.9	13.0	14.6	15.4
120	2.9	0.0	27.9	16.1	9.9	10.5	13.1	14.4	13.6	11.7	13.5	14.6
100	4.9	0.0	24.4	19.6	8.1	8.6	13.2	12.9	12.6	12.1	12.8	13.0
80	13.3	0.0	16.6	20.1	12.2	9.4	13.7	13.3	12.8	12.7	14.9	15.4
60	13.8	0.0	17.5	24.5	18.1	16.6	17.4	15.5	16.1	48.8	72.6	69.9

show that the L_{RMS} norm of the differences obtained in the last iteration performed is a completely inadequate iterative error estimator. The L_∞ norm is definitely a better choice, but its performance tends to degrade with the increase of the grid refinement.

4.7. Discretization error estimation

One of the main goals of this study is to investigate the influence of the iterative error on the estimation of the discretization error/uncertainty.

At the 19×19 nodes, common to all grids, we have estimated the discretization error with the procedure described in Section 2 for the 12 levels of e_t tested. Three different grid refinement levels were selected:

(1) The finest grid, 401×401, with the discretization uncertainty, U_d, based on the 11 finest grids covering a grid refinement ratio of 2 (coarsest grid 201×201).
(2) The 201×201 grid with U_d based on six grids covering a grid refinement ratio of 2 (coarsest grid 101×101).
(3) The 121×121 grid with U_d based on four grids covering a grid refinement ratio of 2 (coarsest grid 61×61).

We have restricted our evaluation of the discretization error estimation procedure and the influence of the iterative error to locations where $U_d > 10^{-7}$. The percentage of grid nodes where this criterion is met is designated by $F(N_d)$.

From the data obtained in these N_d locations, we have computed the following quantities:

- The maximum, minimum and mean values of the ratio between the estimated discretization uncertainty, U_d, and the discretization error, e_{de}, obtained from the difference between the solution converged to machine accuracy and the exact solution.
- The percentage of locations where $U_d < e_{de}, F(U_d)$.
- The percentage of locations where the convergence is monotonic, $F(Mon)$.
- The maximum, minimum and mean values of the observed order of accuracy, p, at the locations where the convergence is monotonic.
- The percentage of locations with monotonic convergence where $1.9 < p < 2.1, F(p_t)$.

The percentage of grid nodes where $U_d > 10^{-7}$ is greater than 75% in all the cases tested. Reasonably, U_d decreases with the grid refinement and so the lowest values of $F(Nd)$ are obtained for the finest grid, $NX = 401$. However, for the largest values of e_t, the iterative error makes U_d increase and $F(Nd)$ is 100% for all the flow variables.

Figs. 2 and 3 present minimum and medium values of U_d/e_{de} as a function of e_t. The estimated discretization uncertainties exhibit a significant influence of the iterative error for the highest levels of

e_t. In general, the rise of the iterative error to non-negligible levels leads to an increase of the estimated U_d, growing roughly linearly with the iterative error (the slope of the mean value of U_d/e_{de} is close to 1 in Fig. 3). This means that the U_d estimations become too conservative. It is also clear that the smallest level of e_t (and consequently of the iterative error) affecting the estimation of U_d depends on the level of the discretization error.

Fig. 4 presents the percentage of grid nodes where $U_d < e_{de}$, $F(Ud)$, for u_x, u_y and C_p as a function of e_t. The results show that it is not guaranteed that U_d increases at all the grid nodes with the rise of the iterative error. The largest percentage of failures to bound the discretization error is obtained for the 201×201 grid and $e_t = 10^{-5}$, which as illustrated in Figs. 2 and 3 already includes the influence of the iterative error on the estimation of the discretization uncertainty. In this case, the level of $F(U_d)$ does not reach 5%. However, for a similar exercise performed with the manufactured eddy-viscosity included in[22], $F(U_d)$ reaches 26% for C_p with $e_t = 10^{-4}$.

The percentage of locations where the convergence is monotonic, $F(Mon)$ is plotted in Fig. 5. The data show that the level of e_t has a drastic influence on the number of locations with apparent monotonic convergence. For negligible values of the iterative error, $e_{im}, F(Mon)$ is close to 100% for the three flow variables. The increase of e_{im} to non-negligible levels causes a significant reduction of the percentage of grid nodes with observed monotonic convergence. The effect is clearly dependent on the level of U_d, because $F(Mon)$ shows the strongest influence of e_{im} for the 401×401 grid and the weakest for the 121×121 grid.

These results suggest that the insufficient reduction of the iterative error makes the use of Richardson extrapolation problematic, because it can change significantly the observed order of accuracy. As a consequence, most values of U_d are estimated from the data range, which is obviously dependent on the iterative error. Furthermore, Richardson extrapolation also magnifies iteration error (and round-off error) [7].

Fig. 6 presents the mean value of p at the locations where u_x, u_y and C_p exhibit monotonic convergence as a function of e_t. The effect of the iterative error on the determination of the observed order of accuracy is evident. For the largest values of e_t, the percentage of locations with p close to the theoretical order of the method drops drastically (see Fig. 7 below) and the mean value obtained for p behaves almost randomly.

It should be mentioned that for the solutions with no influence of the iterative error, the minimum and maximum values of the estimated values of p are strongly dependent on the grid refinement. Table 3 contains the minimum, maximum and mean estimated values of p for the flow fields converged to machine

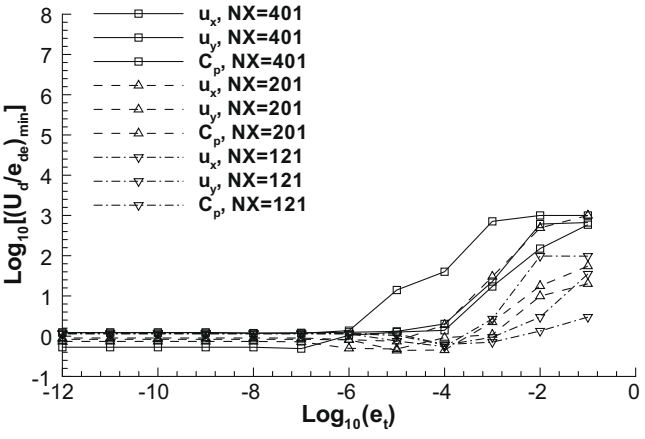

Fig. 2. $\mathrm{Log}_{10}((U_d/e_{de})_{min})$ of u_x, u_y and C_p as a function of the convergence criteria, e_t.

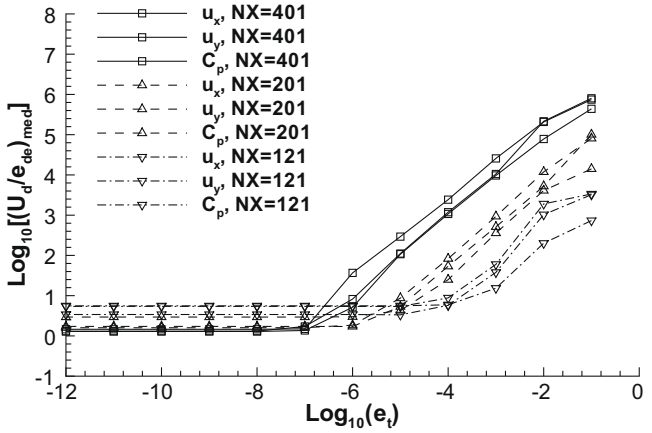

Fig. 3. $\mathrm{Log}_{10}((U_d/e_{de})_{min})$ of u_x, u_y and C_p as a function of the convergence criteria, e_t.

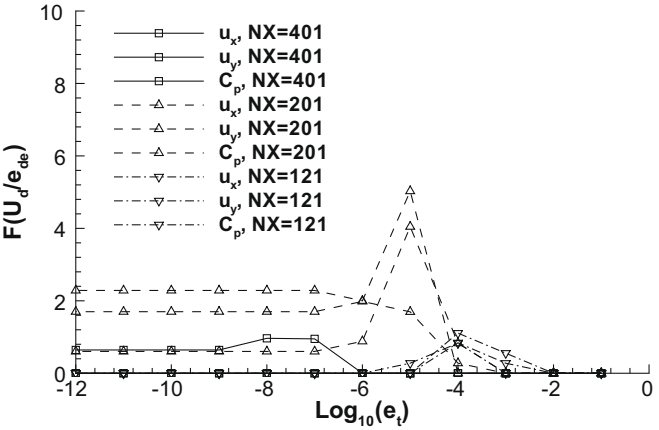

Fig. 4. Percentage of grid nodes where $U_d < e_{de}$ for u_x, u_y and C_p as a function of the convergence criteria, e_t.

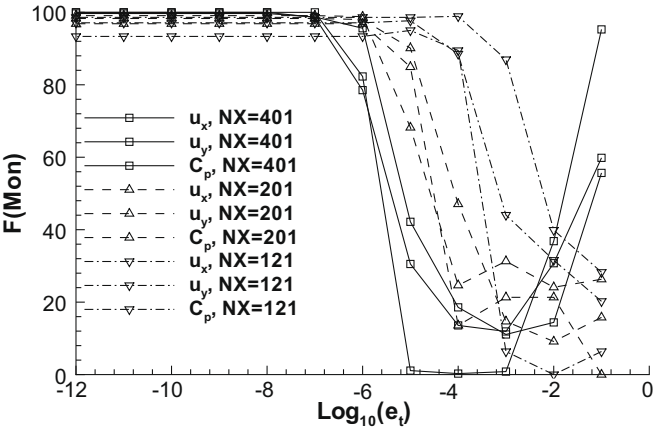

Fig. 5. Percentage of locations where the convergence is monotonic, $F(Mon)$, for u_x, u_y and C_p as a function of the convergence criteria, e_t.

accuracy. The p_{med} of u_y and C_p is close to 2 in the three grids, but for u_x only the finest grid yields p_{med} almost equal to 2. However, the minimum and maximum estimated values of p deviate significantly from 2 even in the 401×401 grid (especially for u_x) and exhibit unreasonably low or high values for the two coarsest grids. This is a clear indication that part of the data used to estimate p in the coarsest grids is not in the asymptotic range.

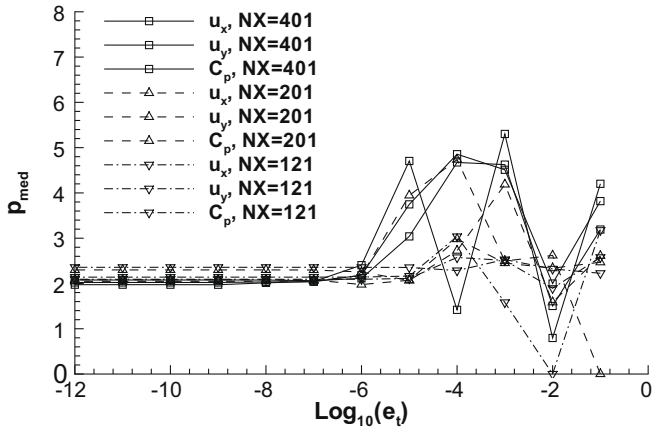

Fig. 6. Mean observed order of accuracy, p_{med}, at the locations with monotonic convergence of u_x, u_y and C_p as a function of the convergence criteria, e_t.

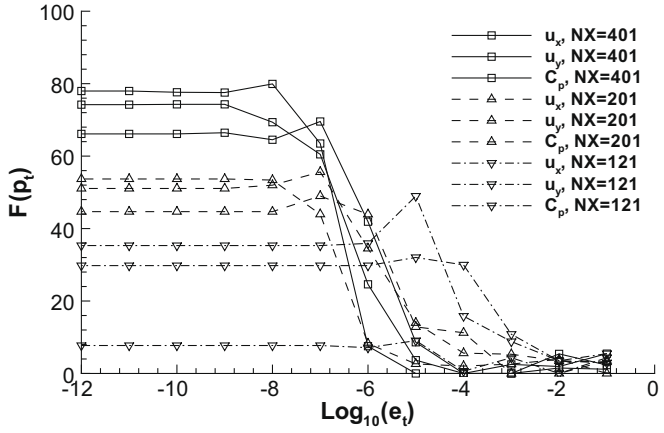

Fig. 7. Percentage of locations where $1.9 < p < 2.1, F(p_t)$, for u_x, u_y and C_p as a function of the convergence criteria, e_t.

Table 3
Minimum, maximum and mean estimated observed order of accuracy of u_x, u_y, and C_p of the solutions converged to machine accuracy.

Grids	u_x			u_y			C_p		
	p_{min}	p_{max}	p_{med}	p_{min}	p_{max}	p_{med}	p_{min}	p_{max}	p_{med}
401×401	0.6	3.7	2.1	1.2	2.8	2.0	1.0	2.2	2.0
201×201	0.7	7.9	2.3	0.1	4.6	2.0	0.4	7.9	2.0
121×121	0.1	7.9	2.4	0.1	5.1	2.1	0.1	7.2	2.1

Fig. 7 presents the percentage of grid nodes with $1.9 < p < 2.1$, $F(p_t)$, as a function of the convergence tolerance, e_t. As expected, $F(p_t)$, increases significantly with the grid refinement. But the results depend on the flow variable selected. For example, for the estimates with no influence of the iterative error, C_p gives the lowest value of $F(p_t)$ in the coarsest grid (only 7.7%) and the highest value for the finest grid (78%). Fig. 7 also shows that most of the locations exhibiting monotonic convergence for the highest values of e_t (a small percentage as illustrated in Fig. 5) do not have an estimated p close to the theoretical order of the method.

In summary, the rule of thumb suggested in [10] that the iterative error should be reduced two to three order of magnitude below the level of the discretization error to have a negligible influence on the estimation of U_d is also verified in this study.

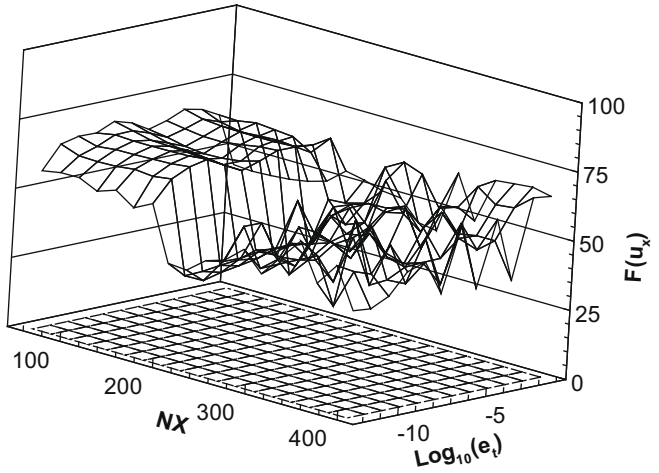

Fig. 8. Percentage of grid nodes where the combination of the iterative and discretization errors is smaller than the numerical error for the horizontal velocity component, u_x, as a function of the number of grid nodes per direction, NX, and the convergence criteria, e_t.

4.8. Combining iterative and discretization errors

In order to investigate the most appropriate way to combine the contributions of the iterative and discretization errors to the numerical error, we have estimated separately the iterative and discretization errors using the solution converged to machine accuracy and the exact solution. The two alternatives (15) and (16) were tried.

The percentage of grid nodes where the estimation of the numerical error is smaller than the true numerical error is illustrated in Figs. 8 and 9 for the two Cartesian velocity components as a function of NX and e_t. This gives a variety of results with cases where the discretization error is dominant (coarsest grids with lowest e_t) and other cases where the iterative error is the main component of the numerical error (finest grids with largest e_t).

Most of the percentages of failure obtained combining the two sources of error by RMS are significantly larger than 5% with most of the cases above 50%. Furthermore, the percentage of fail-

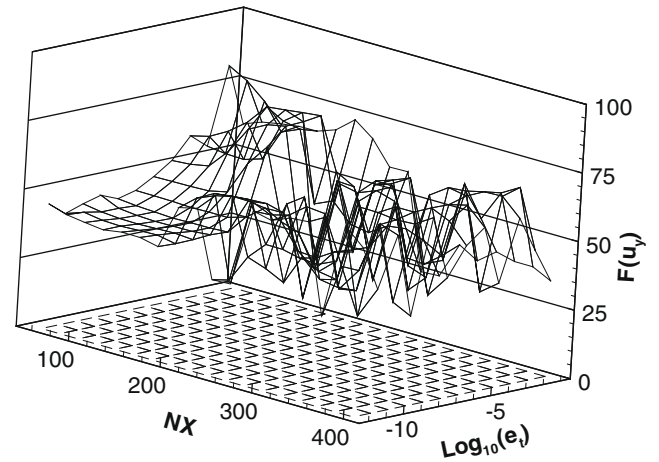

Fig. 9. Percentage of grid nodes where the combination of the iterative and discretization errors is smaller than the numerical error for the vertical velocity component, u_y, as a function of the number of grid nodes per direction, NX, and the convergence criteria, e_t.

ure does not show any change with the grid refinement (discretization error) or convergence tolerance level (iterative error). On the other hand, adding the two contributions arithmetically gives consistently 0 failures for all the cases tested. These results strongly suggest that the underlying assumption of [24], that the contributions of iterative error and computed discretization error are uncorrelated – a common statistical assumption for engineering practice – is not justifiable in this case; it leads to overly optimistic combinations. (Note that the true discretization error could be computed only with complete convergence and no round-off errors.) Thus, combining by RMS is not conservative. The appropriate choice for obtaining a reliable numerical uncertainty is to add the contributions of iterative and discretization error simply arithmetically.

5. Conclusions

In this article we have presented a study on the estimation of the numerical uncertainty based on grid refinement studies with the method of the manufactured solutions. The availability of an exact solution and the numerical solution converged to machine accuracy allowed the calculation of the exact error and of the distinct contributions of the iterative and discretization errors.

For a given grid and convergence criterion we have:

- The difference between an intermediate numerical solution and the exact solution gives the numerical error.
- The difference between an intermediate numerical solution and the solution converged to machine accuracy gives the iterative error.
- The difference between the solution converged to machine accuracy and the exact solution gives the discretization error.

The study focused on three different problems of error/uncertainty (the uncertainty is this case is the error multiplied by a safety factor) estimation:

(1) The estimation of the iterative error/uncertainty.
(2) The influence of the iterative error on the estimation of the discretization error/uncertainty.
(3) The combination of the iterative and discretization contributions to the numerical error/uncertainty.

The calculations were performed on a set of 18 geometrically similar grids with the finite-difference version of PARNASSOS, which is theoretically second-order accurate. Double precision is adopted for all the calculations to ensure that the round-off error is negligible.

The iterative error/uncertainty estimations are based on geometric progression extrapolations of the L_∞ norm or the root mean square of the differences between consecutive iterations, which have the iteration counter as the independent variable. The discretization uncertainty estimations are performed with a procedure that combines a least-squares version of the Grid Convergence Index with the data range. Two alternatives are tested for the combination of the iterative and discretization contributions to the numerical error: the square root of the sum of the iterative and discretization errors squared; the sum of the two error components.

The results lead to the following conclusions:

- The estimation of the iterative error based on the geometric-progression extrapolation of the L_∞ norm of the maximum difference between consecutive iterations is a reliable iterative error estimator. The use of a 1.25 factor of safety guaranteed a banded value of the iterative error for almost all cases tested. The exceptions occurred for unreasonably high values of the tolerance of the convergence criterion.
- The iterative error must be reduced two to three orders of magnitude below the discretization error to guarantee a negligible influence on the estimation of the discretization error. If not, the application of Richardson extrapolation is drastically impaired by the iterative error.
  - The observed convergence properties show a significant decrease of the locations exhibiting monotonic convergence. As a consequence, the discretization error estimation must rely on the data range, which is clearly dependent on the iterative error.
  - In general, the computed discretization uncertainty tends to increase with the iterative error. This leads to overly conservative estimates (mostly due to the use of the data range), which are not welcomed but acceptable. However, the opposite can occur and in that case the discretization uncertainty estimation may fail to meet its goals due to the level of the iteration error.
- The contributions of the iterative and discretization error/uncertainty to the numerical error/uncertainty should be added arithmetically (not in an RMS sense) to obtain a reliable numerical error/uncertainty.

Acknowledgement

The authors acknowledge the helpful discussion and suggestions of Patrick J. Roache in the preparation of this article.

References

[1] Guide for the verification and validation of computational fluid dynamics simulations, AIAA-G077-1998.
[2] ERCOFTAC Special Interest Group on Quality and Trust in Industrial CFD. Best practice guidelines, version 1.0; January 2000.
[3] Guide for the verification and validation in computational solid mechanics – ASME V&V 10, ASME Books 2006, ISBN #: 079183042X.
[4] ASME. Standard for verification and validation in computational fluid dynamics and heat transfer, ASME V&V 20-2008. Am Soc Mech Eng, in press.
[5] Wang SSY, Roache PJ, Schmalz RA, Jia Y, editors. Verification and validation of 3D free-surface flow models. ASCE; 2009.
[6] ITTC quality manual.
[7] Roache PJ. Verification and validation in computational science and engineering. Albuquerque, New Mexico: Hermosa Publishers; 1998.
[8] Eça L, Hoekstra M (Eds.), Proceedings of the workshop on CFD uncertainty analysis, Lisbon; October 2004.
[9] Eça L, Hoekstra M, Roache PJ. Verification of calculations: an overview of the lisbon workshop. In: AIAA computational fluid dynamics conference, Toronto; June 2005. AIAA Paper 4728.
[10] Eça L, Hoekstra M. On the influence of the iterative error in the numerical uncertainty of ship viscous flow calculations. In: 26th Symposium on naval hydrodynamics, Rome, Italy; September 2006.
[11] Pelletier D, Roache PJ. CFD code verification and the method of the manufactured solutions. In: 10th Annual conference of the CFD society of Canada, Windsor, Ontario, Canada; June 2002.
[12] Pelletier D, Roache PJ. Verification and validation in computational, heat transfer handbook of numerical heat transfer. 2nd ed. New York: Wiley; 2006 [chapter 3].
[13] Oberkampf WL, Blottner FG, Aeschliman DP. Methodology for computational fluid dynamics code verification/validation. In: AIAA 26th fluid dynamics conference, San Diego, California; June 1995. AIAA Paper 95-2226.
[14] Turgeon É, Pelletier D. Verification and validation of adaptive finite element method for impingement heat transfer. J Thermophys Heat Transfer 2001;15:284–92.
[15] Turgeon É, Pelletier D. Verification and validation in CFD using an adaptive finite element method. Can Aeronaut Space J 2002;48:219–31.
[16] Knupp P, Salari K. Verification of computer codes in computational science and engineering. Boca Raton, FL: CRC Press; 2002.
[17] Roache PJ. Code verification by the method of the manufactured solutions. ASME J Fluids Eng 2002;114(March):4–10.
[18] Eça L, Hoekstra M, Hay A, Pelletier D. A manufactured solution for a two-dimensional steady wall-bounded incompressible turbulent flow. Int J CFD 2007;21(3–4):175–88.

[19] Eça L, Hoekstra M. On the influence of grid topology on the accuracy of ship viscous flow calculations. In: Fifth Osaka colloquium on advanced CFD applications to ship flow and hull form design, Osaka, Japan; 2005.
[20] Roache PJ. Error bars for CFD. In: 41th aerospace sciences meeting, Reno NV,;January 2003. AIAA-2003-048.
[21] Ferziger JH, Peric M. Computational methods for fluid dynamics. Berlin: Springer-Verlag; 1996.
[22] Eça L, Hoekstra M. Evaluation of numerical error estimation based on grid refinement studies with the method of the manufactured solutions, IST Report D72-42; May 2007.
[23] Eça L, Hoekstra M. An evaluation of verification procedures for cfd applications. In: 24th symposium on naval hydrodynamics, Fukuoka, Japan; July 2002.
[24] Stern F, Wilson R, Coleman HW, Paterson EG. Comprehemsive approach to verification and validation of CFD simulations. Part 1: Methodologies and procedures. ASME J Fluids Eng 2001;123:803–10.
[25] Eça L, Hoekstra M, Hay A, Pelletier D. On the construction of manufactured solutions for one and two-equation eddy-viscosity models. Int J Numer Methods Fluids 2007;54:119–54.
[26] Wilcox DC. Reassessment of the scale-determining equation for advanced turbulence models. AIAA J 1988;26(11):1299–310.
[27] Wilcox DC. Turbulence modeling for CFD. 3rd ed. La Canada: DCW Industries; November 2006.
[28] Menter FR. Two-equation eddy-viscosity turbulence models for engineering applications. AIAA J 1994;32:1598–605.
[29] José MQB, Jacob JMQB, Eça L. 2-D Incompressible steady flow calculations with a fully coupled method. In: VI congresso nacional de mecânica aplicada e computacional, Aveiro; April 2000.
[30] Eça L, Hoekstra M. Discretization uncertainty estimation based on a least squares version of the grid convergence index. In: 2nd Workshop on CFD uncertainty analysis, Instituto Superior Técnico, Lisbon; October 2006.
[31] Vinokur M. On one-dimensional stretching functions for finite-difference calculations. J Comput Phys 1983;50:215–34.
[32] Salas MD. Some observations on grid convergence. Comput Fluids 2006;35(7):688–92.